Ecological Indicators 52 (2015) 411–421

Contents lists available at ScienceDirect

Ecological Indicators

journal homepage: www.elsevier.com/locate/ecolind

Spatiotemporal variations of T/ET (the ratio of transpiration to evapotranspiration) in three forests of Eastern China

Xian-Jin Zhu[a], Gui-Rui Yu[a,*], Zhong-Min Hu[a], Qiu-Feng Wang[a], Hong-Lin He[a], Jun-Hua Yan[b], Hui-Min Wang[a], Jun-Hui Zhang[c]

[a] *Synthesis Research Center of Chinese Ecosystem Research Network, Key Laboratory of Ecosystem Network Observation and Modeling, Institute of Geographic Sciences and Natural Resources Research, Chinese Academy of Sciences, Beijing 100101, China*
[b] *South China Botanical Garden, Chinese Academy of Sciences, Guangzhou 510650, China*
[c] *Institute of Applied Ecology, Chinese Academy of Sciences, Shenyang 110016, China*

ARTICLE INFO

Article history:
Received 20 August 2014
Received in revised form 3 December 2014
Accepted 29 December 2014

Keywords:
Eddy covariance
Shuttleworth–Wallace model
Evapotranspiration
The ratio of transpiration to evapotranspiration (T/ET)
Forest

ABSTRACT

Evapotranspiration (ET), which is comprised by evaporation from soil surface (E), transpiration (T) and evaporation from the intercepted water by canopy (EI), plays an important role in maintaining global energy balance and regulating climate. Quantifying the spatiotemporal variations of T/ET (the ratio of T to ET) can improve our understandings on the role of vegetation ecophysiological processes in climate regulation. Using eddy covariance measurements at three forest ecosystems (Changbaishan temperate broad-leaved Korean pine mixed forest (CBS), Qianyanzhou subtropical coniferous plantation (QYZ) and Dinghushan subtropical evergreen mixed forest (DHS)) in north–south transect of Eastern China (NSTEC), we run the revised Shuttleworth–Wallace model (S–W model), validated its performance with the water vapor fluxes measured at two layers, and quantified the spatiotemporal variations of T/ET. The S–W model performed well in simulating ET and T/ET. The mean value of annual T/ET at three forests during the observation period all exceeded 0.6. The diurnal variation of canopy stomal conductance (G_c) dominated that of T/ET. The seasonal dynamics of T/ET was mainly shaped by that of leaf area index (LAI), vapor pressure deficit (VPD) and air temperature (T_a) through altering G_c and the portion that the energy absorbed by canopy (P_{EC}) at temperate forest (CBS), while the seasonal dynamics of T/ET at subtropical forests (QYZ and DHS) were mainly affected by T_a, net radiation, VPD, and soil water content through altering G_c and soil surface conductance (G_s). The variation of mean annual G_c governed the interannual varaition and spatial variation of T/ET. Therefore, forests in Eastern China played an important role in regulating climate through T and G_c primarily affected the spatial and temproal variations of the role of forest T in regulating climate.

1. Introduction

Forest, occupying 31% of the land surface, plays an important role in global mass cycles and energy flows (FAO, 2010). Evapotranspiration (ET) of forest, an important component sustaining the forest water and energy balance (Falge et al., 2005), affects the global energy partition and then climate, whereas ET is comprised by multiple source water vapor fluxes such as evaporation from soil surface (E), transpiration by plant (T) and evaporation from the intercepted water by canopy (EI) (Kool et al., 2014), which are controlled by different biotic and physical processes (Scanlon and Kustas, 2012). Therefore, to fully clarify the role of each process in forest ET and then in regulating climate, it is critical to quantify the portion of ET components in ET and reveal factors controlling these portions (Hu et al., 2009; Lawrence et al., 2007).

The ratio of T to ET (T/ET), the key parameter for productivity and water use efficiency (Hu et al., 2008; Schlesinger and Jasechko, 2014), reflects the role of vegetation ecophysiological processes in water loss through ET (Hu et al., 2009), which is also a parameter indicating the role of plant ecophysiological processes in regulating climate. The variation of T/ET and its affecting factors have been extensively investigated (Hu et al., 2009; Kato et al., 2004), while most studies about the variation of T/ET are conducted in croplands or grasslands (Hu et al., 2009; Kato et al., 2004; Liu et al., 2002), it is still unclear what dominated the spatiotemporal variations of T/ET in forests.

Meanwhile, quantifying T/ET should base on ET partition, which can be fulfilled through various measurements and models (Blyth

* Corresponding author. Tel.: +86 10 64889432; fax: +86 10 64889432.
E-mail address: yugr@igsnrr.ac.cn (G.-R. Yu).

http://dx.doi.org/10.1016/j.ecolind.2014.12.030
1470-160X/

Table 1
Site descriptions.

Sites	CBS	QYZ	DHS
Latitude (°N)	42.4025	26.7330	23.1670
Longitude (°E)	128.0928	115.05	112.5330
Elevation (m.a.s.l.)	738	100	300
Mean annual temperature (°C)[a]	3.6	17.9	21.0
Mean annual precipitation (mm)[a]	696	1485	1956
Stand age (years)	~200	~23	~100
Dominated species	*Pinus koraiensis*, *Tilia amurensis*, *Acer mono*, *Fraxinus mandshurica*, *Quercus mongolica*	*Pinus elliottii*, *Pinus massoniana*, *Cunninghamia lanceolata*	*Castanopsis chinensis*, *Schima superba*, *Cryptocarya chinensis*, *Cryptocarya concinna*, *Machilus chinensis*
Canopy height (m)	26	12	22
Mean diameters at breast height (cm)	~ 23	14.6	7.06
Maximum leaf area index ($m^2\,m^{-2}$)	6.1	5.6	5.6
Sapwood area ($m^2\,hm^{-2}$)	47.88	30.92	36.30
Total biomass ($tC\,hm^{-2}$)	175	106	130
Mean annual total gross primary productivity ($gC\,m^{-2}\,yr^{-1}$)[b]	1338.84	1798.74	1367.26
Mean annual total ecosystem respiration ($gC\,m^{-2}\,yr^{-1}$)[b]	1036.51	1311.22	971.31
Mean annual total net ecosystem productivity ($gC\,m^{-2}\,yr^{-1}$)[b]	302.33	487.51	395.95
Mean annual total evapotranspiration ($kg\,H_2O\,m^{-2}\,yr^{-1}$)[c]	522.35	761.57	706.20

[a] Values are the averages from 1985 to 2005 according to Yu et al. (2008).
[b] Values are the averages from 2003 to 2008 according to Yu et al. (2013).
[c] Values are the averages from 2003 to 2008 according to ChinaFLUX dataset.

and Harding, 2011; Kool et al., 2014). Shuttleworth–Wallace model (S–W model) is the first model designed for ET partition, which is a physically-based combination model based on Penman–Monteith equation (Shuttleworth and Wallace, 1985). S–W model has also been regarded as an accurate model and the foundation of other ET partition models, which provides a validation for other models (Kool et al., 2014) and has been widely used (Hu et al., 2009; Iritz et al., 2001; Kato et al., 2004), while there have been no attempt in using S–W model to partition ET into its components at forests of China, which occupied an important portion in global forests (FAO, 2010).

China has conducted eddy covariance measurements since 2003 at three forests along the north–south transect of Eastern China (NSTEC), which experiences apparent decreasing temperature and precipitation gradients with the increasing latitude (Yu et al., 2008). The continuous flux measurements at three forests along NSTEC, which helps us understand the effects of environmental factors along climate gradients, provides a valuable platform for analyzing the variations of T/ET among different spatiotemporal scales. Using measurements from three forests along NSTEC, we run the S–W model to partition ET into its components and analyzed the variations of T/ET. The specific objectives were: (1) validate the performances of S–W model at forests, (2) quantify the importance of T in ET at forests, (3) reveal factors affecting the spatiotemporal variations of T/ET, and (4) clarify the difference in the effects of various factors on the spatiotemporal variations of T/ET along climate gradients.

2. Materials and methods

2.1. Site description and measurements

2.1.1. Site descriptions

We collected data from three ChinaFLUX sites: Changbaishan temperate broad-leaved Korean pine mixed forest (CBS), Qianyanzhou subtropical coniferous plantation (QYZ), and Dinghushan subtropical evergreen mixed forest (DHS). Brief descriptions about these three sites were listed in Table 1. Detailed information can be found in our previous works (Wen et al., 2010; Yan et al., 2013; Yu et al., 2008; Zhang et al., 2006).

2.1.2. Measurement and instruments

At three forests, ecosystem CO_2 and H_2O flux data were determined from the open-path eddy covariance system (OPEC) above the canopy with a sampling frequency of 10 Hz and block averaging over 30 min. The OPEC was consisted of an open-path infrared gas analyser (Model LI-7500; Licor Inc., Lincoln, NB, USA), a 3-D sonic anemometer (Model CSAT3; Campbell Scientific Inc., Logan, UT, USA), and a datalogger (Model CR5000; Campbell Scientific Inc.). The measuring height of ecosystem CO_2 and H_2O fluxes for CBS, QYZ, and DHS were 40 m, 39 m, and 27 m, respectively. In addition, another OPEC was installed below the canopy and the measuring height were all around 2.5 m for these three forests.

Routine meteorological variables were measured simultaneously with CO_2 and H_2O fluxes. Global radiation (R_g) and net radiation (R_n) above the canopy were measured with radiometers (Model CM11 and Model CNR-1, Kipp & Zonnen, Delft, Netherlands). Photosynthetic active radiation (PAR) above the canopy was measured with a quantum sensor (Model LI190SB, LICOR Inc.), whereas that below the canopy was measured by five quantum sensors (Model LQS7010-SUN, APOGEE, Logan, UT, USA). Air temperature (T_a) and relative humidity (RH) at different heights above and within canopy were measured with shielded and aspirated probes (Model HMP45C, Campbell Scientific Inc.). Precipitation was recorded with a rain gauge (Model 52203, Rm Young, Traverse City, MI, USA) above the canopy. Soil temperature (T_s) and soil water content (S_{wc}) were measured using thermocouple probes (Model 105T, Campbell Scientific Inc.) and water content reflectometers (Model CS616, Campbell Scientific Inc.), respectively. Soil heat flux (G) was measured with two flux plates (Model HFP01SC, Campbell Scientific Inc.) at the depth of 5 cm. All micrometeorological measurements were recorded at 30-min intervals with dataloggers (Model CR10X & CR23X, Campbell Scientific Inc.). The detailed equipment descriptions were also described by previous works (Wen et al., 2010; Yan et al., 2013; Yu et al., 2008; Zhang et al., 2006).

Leaf area index (LAI) was measured at two-week intervals or a longer period during the growing seasons from 2003 to 2005 using a canopy analyzer (Model LAI-2000, LICOR Inc.).

2.2. Data preparing

Flux data measured by eddy covariance technique in two layers (above and below the canopy) were subjected to traditional data quality control routes including three-dimensional rotation (Aubinet et al., 2000), WPL (Webb, Pearman and Leuning) correction (Webb et al., 1980), storage calculation (Hollinger et al., 1994), and spurious data removal caused by rainfall, water condensation, system failure, low turbulence and so on. The u^* threshold for determining the low turbulence fluxes was calculated following Reichstein et al. (2005) for two layer fluxes based on u^*, CO_2 fluxes, and T_a. Following Menzel et al. (2003), we determined the start and the end of growing-season based on daily T_a. Negative CO_2 fluxes at nighttime (when the solar elevation angle was lower than 0°) and at non-growing season were then also removed. After data quality control, the average data coverage during 2003 to 2009 was 54%, 46%, and 43% for CBS, QYZ, and DHS, respectively, while that at daytime was 73%, 77%, and 64%, respectively.

For CO_2 fluxes measured above and below the canopy, if data gaps were less than 2 h, they were linearly interpolated. For other gaps, the missing daytime CO_2 fluxes were interpolated using the Michaelis–Menten equation with PAR (Falge et al., 2001b), whereas the missing nighttime CO_2 fluxes were filled using the Lloyd–Taylor model with T_s at 5 cm depth following previous studies (Gao et al., 2014; Reichstein et al., 2005). Daytime ecosystem respiration (Re) was calculated with the trained Lloyd–Taylor model at nighttime having T_s at 5 cm depth as the input variable (Gao et al., 2014; Reichstein et al., 2005). Half-hourly gross primary productivity (GPP) values were obtained based on the calculated daytime Re and the filled half-hourly daytime CO_2 fluxes. For the two layer H_2O fluxes, data gaps were filled by the look-up table method (Falge et al., 2001a; Reichstein et al., 2005) based on T_a, vapor pressure deficit (VPD), and R_n.

Data gaps of meteorological variables (including R_n, T_a, $S_{\rm wc}$, and so on) were filled with the mean diurnal variation (MDV) method for longer periods but using the linear interpolation for gaps of less than 2 h (Falge et al., 2001b). Based on the measured RH and T_a, VPD was then calculated as the difference between the actual and saturation vapor pressures.

Based on PAR measured above and within the canopy, we calculated the absorbed PAR. Daily LAI was estimated from integrating the absorbed PAR with the relationship between the absorbed PAR and LAI, which was established by the absorbed PAR at 12:00 pm and the measured LAI (Beer et al., 2009; Gower et al., 1999; Law et al., 2001).

2.3. Model description and parameterizations

2.3.1. Model descriptions

S–W model was firstly developed based on the Penman–Monteith model and regarded ET as the sum of two water vapor fluxes from separate sources: evaporation from the soil surface (E) and transpiration from the canopy (T) (Shuttleworth and Wallace, 1985). Five resistances were explored in S–W model with units of s m^{-1} (Fig. 1): the soil surface resistance ($r_{\rm ss}$), the aerodynamic resistance from the soil surface to the canopy ($r_{\rm as}$), the canopy stomatal resistance ($r_{\rm sT}$), the bulk boundary layer resistance ($r_{\rm ac}$) and aerodynamic resistance from the canopy to the reference height ($r_{\rm aa}$).

In S–W model, T and E was calculated as:

$$\mathrm{ET} = C_c \mathrm{PM}_c + C_s \mathrm{PM}_s \tag{1a}$$

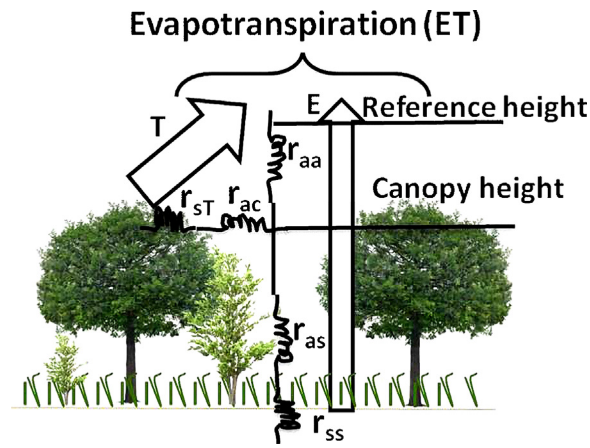

Fig. 1. Evapotranspiration components and their experiencing resistances. T and E were the abbreviations of transpiration and evaporation from the soil surface, respectively. The resistances included: the soil surface resistance ($r_{\rm ss}$), the aerodynamic resistance from the soil surface to the canopy ($r_{\rm as}$), the canopy stomatal resistance ($r_{\rm sT}$), the bulk boundary layer resistance ($r_{\rm ac}$) and aerodynamic resistance from the canopy to the reference height ($r_{\rm aa}$).

$$\mathrm{PM}_c = \frac{\Delta (R_n - G) + \left(\rho C_p \,\mathrm{VPD} - \Delta r_{\rm ac} (R_{\rm ns} - G)\right) / (r_{\rm aa} + r_{\rm ac})}{\Delta + \gamma \left(1 + r_{\rm sT} / (r_{\rm aa} + r_{\rm ac})\right)} \tag{1b}$$

$$\mathrm{PM}_s = \frac{\Delta (R_n - G) + \left(\rho C_p \,\mathrm{VPD} - \Delta r_{\rm as} (R_n - R_{\rm ns})\right) / (r_{\rm aa} + r_{\rm as})}{\Delta + \gamma \left(1 + r_{\rm ss} / (r_{\rm aa} + r_{\rm as})\right)} \tag{1c}$$

where PM_c and PM_s were terms describing T and E, respectively, whereas C_c and C_s were the resistance coefficient for canopy and soil surface, respectively. Δ was the slope of the saturation vapor pressure versus temperature curve (kPa K^{-1}). R_n and $R_{\rm ns}$ (W m^{-2}) were the net radiation arriving at the canopy and the soil surface, respectively. G was the soil heat fluxes (W m^{-2}). ρ was the air density (1.293 kg m^{-3}) and C_p was the specific heat at constant pressure (1012 J kg^{-1} K^{-1}). VPD was the abbreviation of vapor pressure deficit (kPa) and γ was the psychrometric constant (0.067 kPa K^{-1}). $r_{\rm ac}$ was the bulk boundary layer resistance and $r_{\rm aa}$ was aerodynamic resistance from the canopy to the reference height. $r_{\rm ss}$ was the soil surface resistance and $r_{\rm as}$ was the aerodynamic resistance from the soil surface to the canopy. $r_{\rm sT}$ was the canopy stomatal resistance.

C_c and C_s can be drawn as:

$$C_c = \left[1 + \frac{R_c R_a}{R_s (R_c + R_a)}\right]^{-1} \tag{2a}$$

$$C_s = \left[1 + \frac{R_s R_a}{R_c (R_s + R_a)}\right]^{-1} \tag{2b}$$

where R_c, R_a and R_s were given as:

$$\begin{aligned} R_a &= (\Delta + \gamma) r_{\rm aa} \\ R_s &= (\Delta + \gamma) r_{\rm as} + \gamma r_{\rm ss} \\ R_c &= (\Delta + \gamma) r_{\rm ac} + \gamma r_{\rm sT} \end{aligned} \tag{3}$$

$R_{\rm ns}$ was estimated through Beer's law using LAI as:

$$R_{\rm ns} = R_n \times \exp(-k \times \mathrm{LAI}) \tag{4}$$

where k was extinction coefficient, which was set to 0.5 in this study according to previous study (Beer et al., 2009) as the forests were needle forest or mixed forest.

The calculations of each resistances were described in the previous study (Shuttleworth and Wallace, 1985) in detail. In a recent study, Hu et al. (2009) revised the expressions of soil surface resistance (r_{ss}) and the canopy stomatal resistance (r_{sT}). r_{ss} was calculated as the function of soil water content (S_{wc}):

$$r_{ss} = b_1 \left(\frac{S_{ws}}{S_{wc}}\right)^{b_2} + b_3 \tag{5}$$

where S_{ws} was the saturated water content in the surface soil ($m^3\,m^{-3}$), which was set to 0.48, 0.42, and 0.54 for CBS, QYZ, and DHS, respectively. b_1, b_2, b_3 were empirical constants.r_{sT} was calculated using a modified Ball–Berry model (Hu et al., 2009; Wang and Leuning, 1998) as:

$$r_{sT} = \frac{1}{g_0 + a_1 \times f(S_{wc}) \times \mathrm{GPP} \times \mathrm{RH}/C_a} \tag{6a}$$

$$f(S_w) = \frac{S_{wc} - S_{wn}}{S_{wm} - S_{wn}} \tag{6b}$$

where g_0 and a_1 were empirical parameters, and g_0 was set to 0.00001 following Hu et al. (2009). S_{wm} and S_{wn} were the surface soil water content at field capacity and the wilting point, which was set to the observed maximum and the minimum S_{wc}, respectively. C_a was leaf surface CO_2 content, which was calculated from the LI-7500 measurements.

In this study, we run the S–W model following Hu et al. (2009). Moreover, to make the revised S–W model by Hu et al. (2009) more suitable for forests, we revised the calculation of roughness length (z_0) and displacement height (d), which were used for calculating the aerodynamic resistances, following the previous study (Shi et al., 2008b) as:

$$z_0 = 0.075 \times h \tag{7a}$$

$$d = 0.75 \times h \tag{7b}$$

where h was the canopy height.

2.3.2. Model parameterization

The surface resistances, i.e., r_{ss} and r_{sT}, were calculated with Eqs. (5), (6a) and (6b). The empirical parameters (b_1, b_2, b_3, and a_1) in Eqs. (5) and (6a) were estimated using the Monte Carlo method in each year and each site following Hu et al. (2009). In each site and each year, 273 days (about 75% of the whole year data) data were randomly selected to estimate the empirical parameters. In the selected days, only data having high confidence according to Reichstein et al. (2005) were used for training the empirical parameters.

2.4. Data analysis

In this study, we run the S–W model with the trained empirical parameters and validated its performance (including its performances on simulating ET and T/ET) using the independent datasets. The model outputs were then used to analyze the spatiotemporal variations of T/ET.

2.4.1. Model validation

Excluding the 273 days data used for training the model, we selected the remaining 92 (or 93 in 2004 and 2008) day data as the validation dataset to validate the performances of the model. The validation was conducted at two aspects: the performance of S–W model on simulating ET and that on simulating T/ET.

We validated the performance of S–W model on simulating ET at three scales: half-hour scale, daily scale and annual scale. At half-hour scale, the simulated half-hour ET was validated with the high confidence data (Reichstein et al., 2005) in the validation dataset. At daily scale, the validation was conducted at three scenarios. The simulated daily ET was firstly validated with the daily ET in validation dataset after gap-filling. Days in validation dataset having more than 15 high confidence half-hour data at daytime were then selected to validate the simulated corresponding daily ET, which may prevent the effects of gap-fillings. In addition, S–W model was also validated in no rain days to exclude the effects of precipitation on the performance of S–W model. At annual scale, we validated our simulated annual total ET with that measured by eddy covariance after gap-filling.

We validated the performance of S–W model on simulating T/ET through integrating two layer H_2O fluxes measured by eddy covariance: above and below the canopy. H_2O fluxes from the eddy covariance system below canopy can be regarded as E (Wilson et al., 2001). T can therefore be obtained from the difference between H_2O fluxes obtained by two layer eddy covariance measurements. The performance of T/ET was validated at daily and annual scale. The validation of T/ET at daily scale was conducted by grouping ET with the bin width of 0.1 $kg\,H_2O\,m^{-2}\,d^{-1}$ to prevent the effects of random errors in measurements.

2.4.2. Model output analysis

With model outputs of T and ET at half hour scale, we calculated the daily and annual total values. Then T/ET values at half-hour scale, daily scale, and annual scale, which were used to analyze the spatiotemporal variations of T/ET, were calculated with T and ET at the corresponding scales.

With model outputs of the canopy stomatal resistance (r_{sT}) and the soil surface resistance (r_{ss}), we calculated canopy stomatal conductance (G_c) and the soil surface conductance (G_s) as the reciprocal of r_{sT} and r_{ss}, respectively. The annual mean G_c (MG_c) was calculated as the mean daytime G_c during growing season.

To illustrate the way that various factors affecting the variation of T/ET, we also calculated the portion that the energy absorbed by canopy (P_{EC}), which was calculated as the ratio of the energy absorbed by canopy (R_c) to that arrived at the canopy (R_n) from Eq. (4) and can be regarded as the function of LAI:

$$P_{EC} = \frac{R_c}{R_n} = \frac{(R_n - R_{ns})}{R_n} = 1 - \exp(-0.5 \times \mathrm{LAI}) \tag{8}$$

2.5. Statistical analysis

We processed data and run the model with MATLAB software (Math Works Inc., Natick, MA). Under Matlab 7.7, we used the generalized linear model (GLM) of regstats to conduct the regression analysis between simulated and measured values to validate the model performances. With paired-sample T-test, the significance test on the difference between simulated and measured annual T/ET was conducted ($\alpha = 0.05$). We employed the path-analysis to evaluate the dependence of the seasonal dynamics of T/ET on various factors. Then the multivariable regression was conducted to build the equation describing the seasonal dynamics of T/ET. The regressions between T/ET and various factors were also completed with the generalized linear model (GLM) of regstats or nonlinear regressions.

3. Results

3.1. Performances of S–W model

3.1.1. Performance of S–W model on simulating ET

At half-hour scale, the simulated ET by S–W model were well consistent with the measurements, which were the high confidence data in the validation dataset, in three forests (Fig. 2). The slope of the simulated ET: the measured ET were all around 1. The R^2 of the regression between measurements and the simulated ET ranged from 0.59 to 0.72, all of which were significant in statistics.

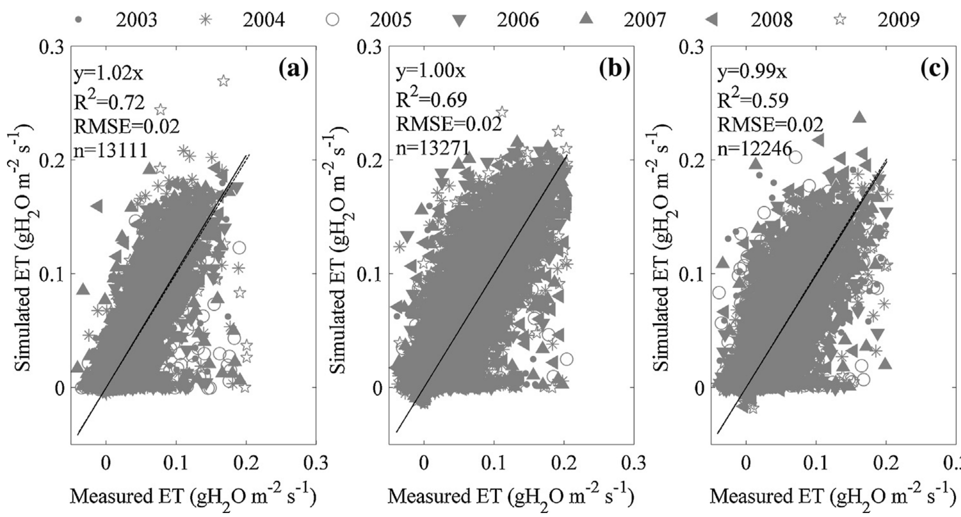

Fig. 2. The performance of Shuttleworth–Wallace model (S–W model) on simulating half-hour evapotranspiration (ET) at CBS (a), QYZ (b), and DHS (c). Measured ET were the high confidence data in the validation dataset, while the Simulated ET were the corresponding ET generated by S–W model. The solid line was the regression line between simulated and measured ET while the dash line was the 1:1 line.

At daily scale, S–W model performed well on simulating ET both in the direction and in the magnitude (Fig. 3). In all three scenarios, the simulated ET were positively correlated with measurements, which were the daily ET at validation dataset, and the R^2 of the regression between the simulated ET and the measurements increased from all validation days to no rain days. The simulated ET agreed well with the measured values in days in validation dataset, which were calculated after gap-filling (Fig. 3a–c). However, in days

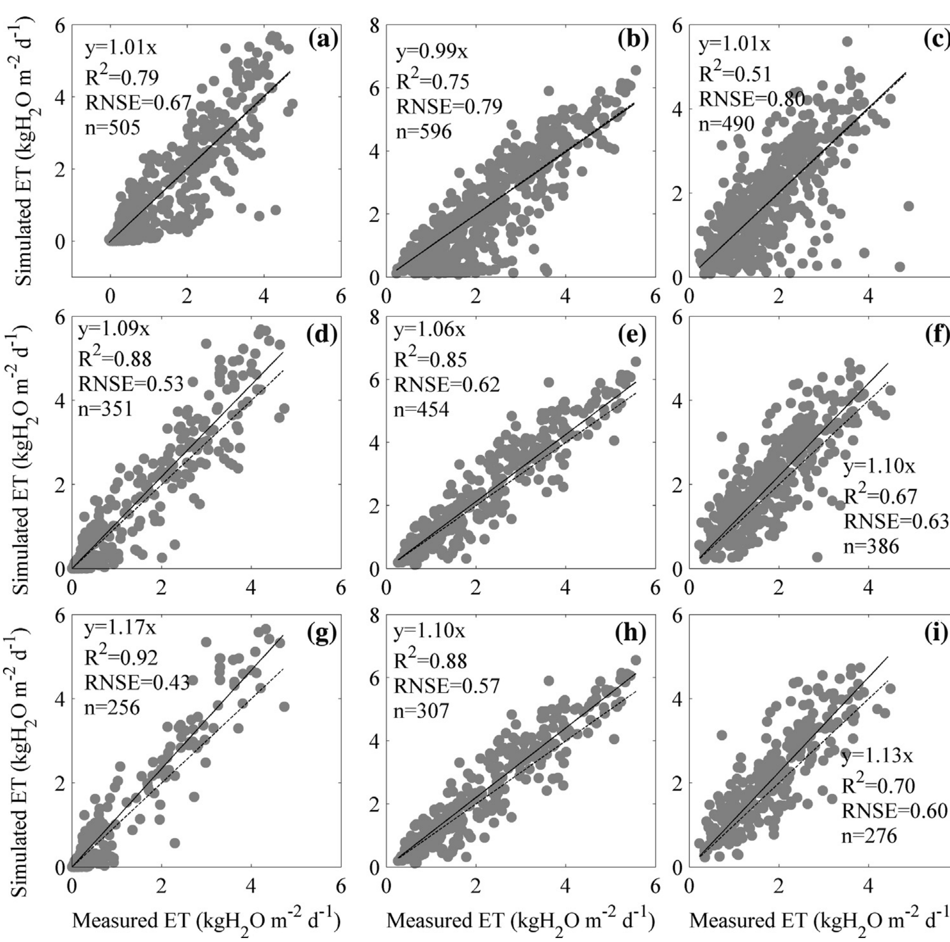

Fig. 3. The performance of Shuttleworth–Wallace model (S–W model) on simulating daily evapotranspiration (ET) at three forests. Measured ET were the measured daily ET at the validation dataset, while the Simulated ET were the corresponding ET simulated by our S–W model. (a–c) were the performance at CBS, QYZ, and DHS, respectively. (d–f) were the performance at CBS, QYZ, and DHS in days in validation dataset having more than 15 half-hour high confidence data at daytime, respectively. (g–i) were the performance at these three sites in no rain days. The solid line was the regression line while the dash line was the 1:1 line.

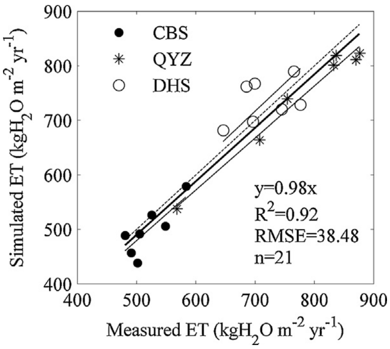

Fig. 4. The performance of Shuttleworth–Wallace model (S–W model) on simulating annual evapotranspiration (ET) at three forests. The solid line was the regression line among site-year data while the dash line was the 1:1 line. The thin solid line was the regression line among years within the same ecosystem.

having more than 15 half-hour high confidence data at daytime and no rain days, the simulated ET slightly overestimated the measurements (Fig. 3d–i).

The high consistency between the simulated ET and the measured ones was also found at annual scale. The simulated annual total ET positively correlated with the measured ET and the values were also comparable (Fig. 4).

Table 2
The measured and simulated annual ratio of transpiration to evaportranspiration (*T*/ET) at three forest ecosystems.

Ecosystem	Year	Measured *T*/ET	Simulated *T*/ET
CBS	2003	0.56	0.67
	2004	0.59	0.69
	2005	0.52	0.68
	2006	0.55	0.78
	2007	0.53	0.55
	2008	0.60	0.68
	2009	0.59	0.73
	Mean (std)	**0.56 (0.03)b**	**0.68 (0.07)a**
QYZ	2004	0.85	0.70
	2005	0.69	0.40
	2006	0.77	0.82
	Mean (std)	**0.77 (0.08)a**	**0.64 (0.22)a**
DHS	2003	0.73	0.73
	2004	0.73	0.56
	2005	0.70	0.54
	2006	0.72	0.54
	Mean (std)	**0.72 (0.01)a**	**0.68 (0.11)a**

Note: Measured *T*/ET were calculated from two layer eddy covariance measured water vapor fluxes. Simulated *T*/ET were obtained from the revised Shuttleworth–Wallace model (S–W model) following Hu et al. (2009). Different lowercase letters between the Measured *T*/ET and Simulated *T*/ET indicated a significant difference at $\alpha = 0.05$ in the same site.

3.1.2. Performance of S–W model on simulating T/ET

At daily scale, S–W model performed well on simulating *T*/ET. The simulated *T*/ET agreed well with the measured ones (Fig. 5a–c), with the R^2 between simulated and measured *T*/ET ranging from 0.36 to 0.76. While the value of our simulated *T*/ET differed from that of measured *T*/ET. At CBS, our simulated *T*/ET were larger than the measured ones when *T*/ET were lower than 0.5 but it was in reverse when *T*/ET were larger than 0.5. At subtropical forests (QYZ and DHS), most simulated *T*/ET were both lower than the measured values. After excluding the effects of precipitation, we found an improved relationship between simulated and measured *T*/ET at CBS, which was indicated by an improved R^2 (Fig. 5d). The relationship between simulated and measured *T*/ET got worse at DHS, whereas most data distributed around the 1:1 line (Fig. 5f).

At annual scale, there were obvious difference between our simulated *T*/ET and the measured values (Table 2). At CBS, our simulated *T*/ET (0.68 ± 0.07) were significantly higher than the measured *T*/ET (0.56 ± 0.03). While at subtropical forests (QYZ and DHS), the simulated *T*/ET were both lower than the measured *T*/ET in values, though the difference between two *T*/ET was not significant in statistics ($p > 0.05$). In addition, our simulated *T*/ET were comparable with published results in temperate and subtropical forests (Granier et al., 2000; Schlesinger and Jasechko, 2014; Stoy et al., 2006).

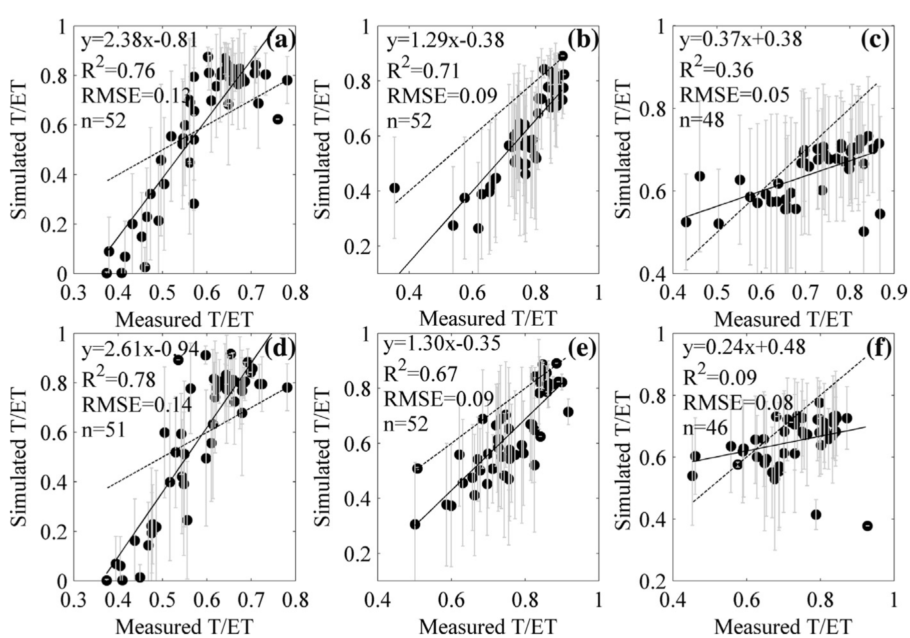

Fig. 5. The performance of Shuttleworth–Wallace model (S–W model) on simulating the ratio of transpiration to evapotranspiration (*T*/ET) at three forests. (a–c) were the performance at CBS, QYZ, and DHS, respectively. (d–f) were the performance at CBS, QYZ, and DHS after excluding data from rainy days, respectively. Data were binned with the measured ET with the bin width of 0.1 kg H_2O m^{-2} d^{-1}. Error bars were the standard deviation of *T*/ET within each group. The solid line was the regression line while the dash line was the 1:1 line.

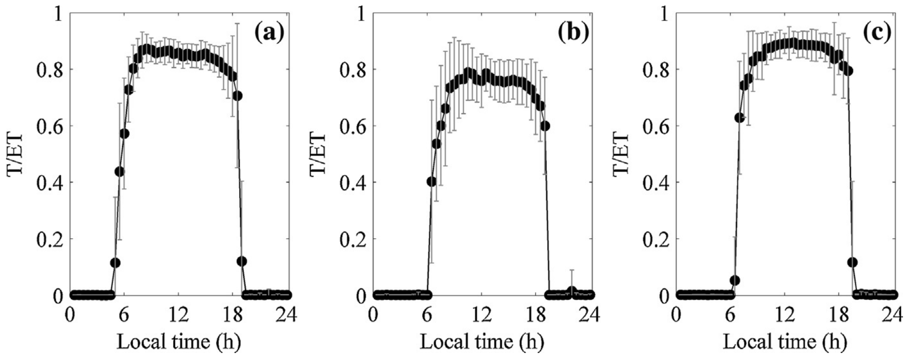

Fig. 6. The diurnal variation of the ratio of transpiration to evapotranspiration (T/ET) at CBS (a), QYZ (b), and DHS (c). Data were collected during August, 2003 from Shuttleworth–Wallace model outputs. Error bars were the standard deviation of T/ET in the same local time.

3.2. Spatiotemporal variations of T/ET

3.2.1. Diurnal variation

With data obtained from the S–W model at August, 2003, we investigated the diurnal variation of T/ET in three forests. T/ET all showed a single-peak diurnal pattern, with the nearly constant T/ET in the daytime while nearly zero in nighttime (Fig. 6), which was also found in other months and years (data were not shown).

The diurnal variation of T/ET was primarily affected by that of canopy stomatal conductance (G_c) (Fig. 7). With the increasing G_c, T/ET showed an obvious increasing trend. The power function based on G_c explained over 90% of variation in T/ET.

3.2.2. Seasonal variation

With data obtained from the S–W model, we found that T/ET exhibited obvious seasonal variations, while the seasonal variation of T/ET differed among forests (Fig. 8). At CBS, T/ET exhibited a single-peak variation and reached its peak value around July, with the value ranging from 0 to 0.85. At QYZ, T/ET also showed a single-peak variation but the range of T/ET obviously narrowed, which only ranged from 0.3 to 0.8 in most years. At DHS, T/ET exhibited an obvious single-peak pattern in most years but the range of T/ET further narrowed.

The seasonal variation of T/ET was shaped by multi-factors through their direct or indirect effects. The direct factors affecting the seasonal dynamics of T/ET differed among forests (Fig. 9). At CBS, the seasonal dynamics of T/ET was mainly affected by the direct effects of T_a, VPD, and LAI. The increase in T_a and LAI directly enhanced T/ET while the increasing VPD exerted a reverse role (Fig. 9a). However, at subtropical forests (QYZ and DHS), LAI played no direct effects on the seasonal variation of T/ET, whereas T_a, S_{wc}, R_n and VPD directly affected the seasonal dynamics of T/ET. With the increasing R_n and T_a, T/ET showed obvious increasing trends, while the increasing S_{wc} and VPD decreased T/ET (Fig. 9b and c).

With the direct factors affecting the seasonal dynamics of T/ET, we drew equations describing the seasonal dynamics of T/ET as follows:

$$\text{CBS}: \frac{T}{\text{ET}} = 0.017T_a - 0.17\,\text{VPD} + 0.13\,\text{LAI} - 0.01, \quad R^2 = 0.87, \quad \text{RMSE} = 0.13, \quad n = 2557 \tag{9a}$$

$$\text{QYZ}: \frac{T}{\text{ET}} = 0.02\,T_a - 0.20\,\text{VPD} - 0.85\,S_{wc} + 0.02R_n + 0.38, \quad R^2 = 0.52, \quad \text{RMSE} = 0.16, \quad n = 2557 \tag{9b}$$

$$\text{DHS}: \frac{T}{\text{ET}} = 0.02T_a - 0.12\,\text{VPD} - 0.44S_{wc} + 0.01R_n + 0.36, \quad R^2 = 0.45, \quad \text{RMSE} = 0.13, \quad n = 2557 \tag{9c}$$

3.2.3. Interannual and spatial variations

Data from S–W model suggest that annual total T occupied a large portion of annual water loss as ET at three forests. During the measuring period, the mean annual value of T/ET for CBS, QYZ, and DHS were 0.68 ± 0.07, 0.65 ± 0.13, and 0.68 ± 0.07, respectively. Therefore, vegetation at NSTEC played an important role in

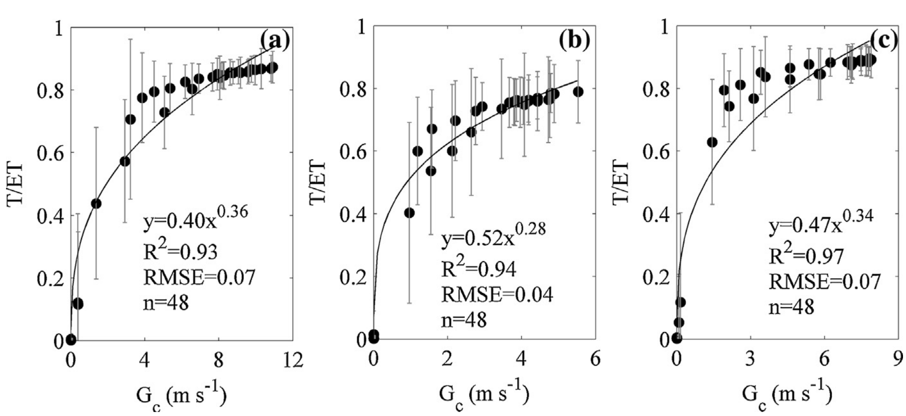

Fig. 7. The effect of canopy stomatal conductance (G_c) on the diurnal variation of the ratio of transpiration to evapotranspiration (T/ET) at CBS (a), QYZ (b), and DHS (c), respectively. Data were obtained from Shuttleworth–Wallace model during August, 2003. Each points indicated the mean value of T/ET at each half-hour and error bars were the standard deviation of T/ET in each half-hour.

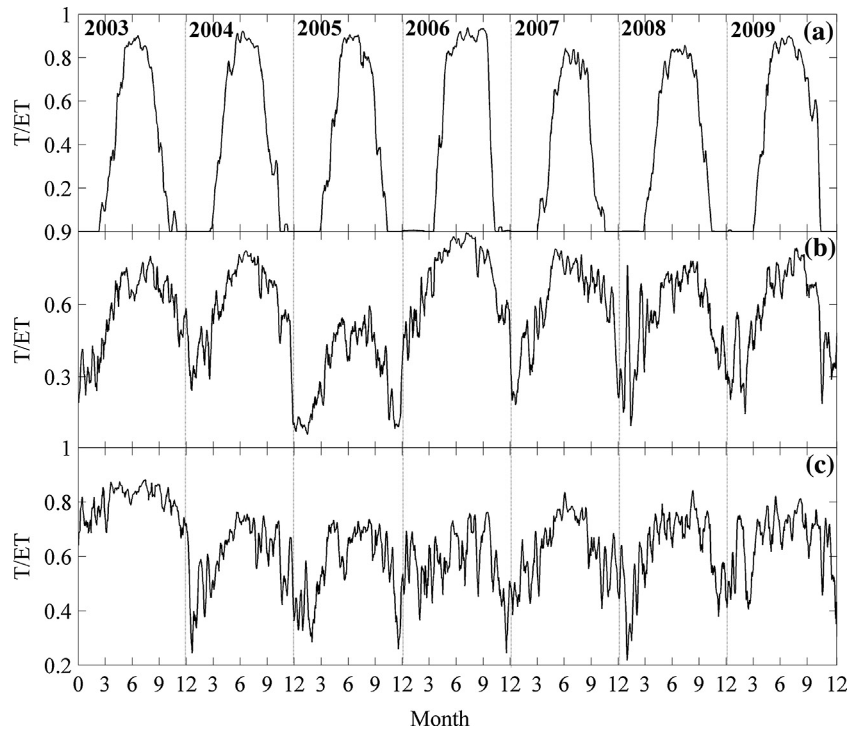

Fig. 8. Seasonal dynamics of the ratio of transpiration to evapotranspiration (*T*/ET) at CBS (a), QYZ (b), and DHS (c). Lines are 10-d running average.

regulating the climate, which should be paid more attention in the future.

T/ET showed obvious interannual variations but was not directly affected by climate and biotic factors such as mean annual air temperature (MAT), mean annual precipitation (MAP), and mean leaf area index (LAI). With the increasing MAT, MAP, and LAI, *T*/ET showed no obvious trend among years (Fig. 10). However, mean canopy stomatal conductance (MG_c) did affect the interannual variation of *T*/ET. With the increasing MG_c, *T*/ET exhibited an obvious increasing trend, which was found at all three forests (Fig. 11).

T/ET also exhibited some differences among forests. *T*/ET in the temperate forest (CBS) was comparable with that at DHS but was slightly higher than that at QYZ. Though *T*/ET showed a slight decreasing trend with the increasing MAT, MAP, and LAI, the relationship between *T*/ET and factors (i.e., MAT, MAP, and LAI) was not significant in statistics (Fig. 10). However, with the increasing MG_c, *T*/ET significantly increased among ecosystems (Fig. 11).

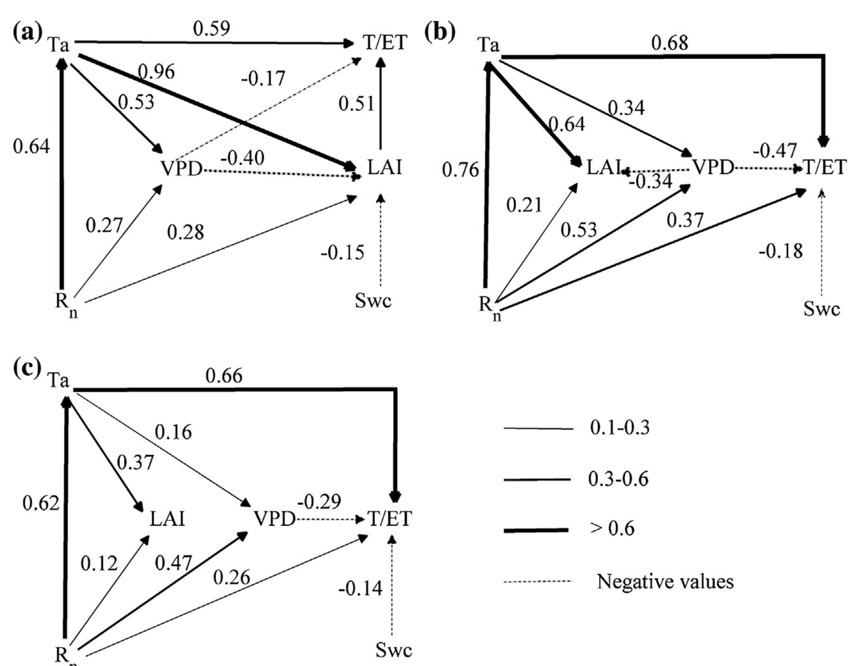

Fig. 9. Path diagram of factors affecting the seasonal dynamics of the ratio of transpiration to evapotranspiration (*T*/ET) at CBS (a), QYZ (b), and DHS (c). The abbreviation of factors were as follows: air temperature (T_a), net radiation (R_n), soil water content (S_{wc}), vapor pressure deficit (VPD), leaf area index (LAI).

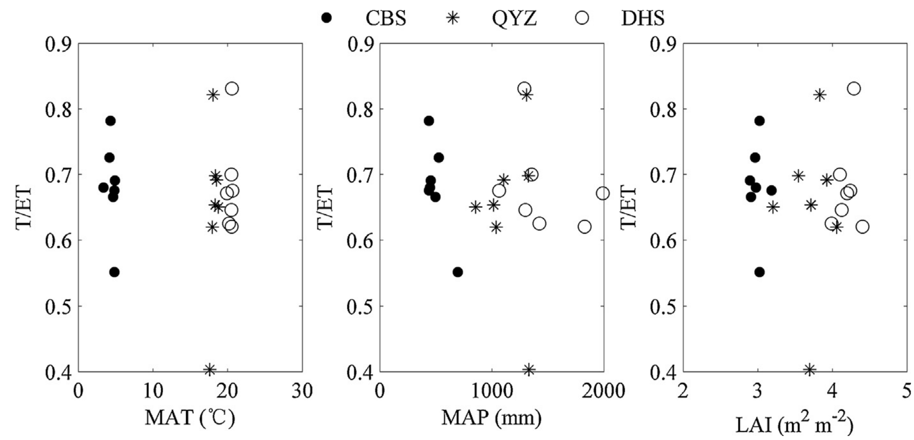

Fig. 10. Factors affecting the ratio of annual total transpiration to annual total evapotranspiration (*T*/ET) at each site. MAT, MAP, and LAI were the abbreviation of mean annual air temperature, mean annual precipitation, and mean leaf area index, respectively.

4. Discussion

4.1. Model performances and uncertainties

Results from model validations suggest that S–W model performed well on simulating the variation trend of ET and *T*/ET (Figs. 2–5), while the simulated ET and *T*/ET differed from the measured ones in values, which can be attributed to the uncertainties in measurements and simulations.

The uncertainties in measurements included the following aspects. First, due to the effects of gap-filling in rainy days (Kang et al., 2012), dews (Maestre-Valero et al., 2012), and fogs (Beiderwieden et al., 2008; Eugster et al., 2006), the measured ET may be underestimated. Second, the underestimated ET caused by gap-filling in rainy days (Kang et al., 2012), dews (Maestre-Valero et al., 2012), and fogs (Beiderwieden et al., 2008; Eugster et al., 2006) may overestimate *T*/ET. Third, during days with open canopy, the low temperature (Shi et al., 2008a) caused small measured water vapor fluxes below the canopy, which made the measured *T* (the difference between two layers water vapor fluxes) and *T*/ET overestimated. Fourth, during days having close canopy, water vapor fluxes measured below the canopy may contribute to *T*, which made the measured *T* and *T*/ET underestimated.

The uncertainties in simulations primarily sourced from the lackage of EI session in S–W model. During the period when the measured ET were directly measured by eddy covariance and had high confidence, EI scarcely occurred. The simulated ET and *T*/ET therefore fully reflected their real values. However, during rainy days or days having much low confidence data, EI appeared but was not simulated by S–W model. The simulation would underestimate the real ET but may overestimate the real *T*/ET.

The consistent high confidence in simulations and measurements made the values of simulated ET agree well with the measured ones at half-hour scale (Fig. 2). The consistent underestimation in simulations and measurements also made the simulated ET agree well with the measured ones at daily and annual scale (Figs. 3a–c and 4), while during days having more than 15 half-hour high confidence data at daytime and no rain days, the single underestimation in the measured ET made the simulated ET higher than the simulated values (Fig. 3d–i). At the temperate forest (CBS) which experienced obvious canopy developments, during days with the open canopy, the overestimation in measured *T*/ET made the simulated *T*/ET lower than the measured ones, while the underestimation in measured *T*/ET primarily accounted for the higher simulated *T*/ET (Fig. 4a and d) during days with the close canopy. The overwhelming portion of growing-season ET in annual total ET (Shi et al., 2008b) also made the simulated annual *T*/ET higher than the measured ones (Table 2). At subtropcial forests, the consistent overestimation in simulations and measurements made the simulated annual *T*/ET be comparable with the measured values (Table 2).

Though there were some uncertainties in the simulated *T*/ET due to the lackage of EI session in S–W model, EI occupied no more than 20% of ET in these three forests. For example, the portion of EI in ET in temperate forest in a forest in Finland (Ge et al., 2011) and Sweden (Iritz et al., 2001) was around 10%, which had similar climate and vegetation status as CBS, while EI occupied about 15.79% of ET at a tropical rainforest (Kume et al., 2011), which had more precipitation than the two subtropical forests but similar vegetation status. In addition, the simulated *T*/ET were comparable with the measured ones (Fig. 5 and Table 2) and those published in literatures. We can therefore conservatively conclude that the overestimation in *T*/ET was relatively small at these three forests. However, to make S–W model more feasible for its application in forests and accurately quantify the portion of each ET components, intergrating an EI session to the S–W model should be paid much attention in the future.

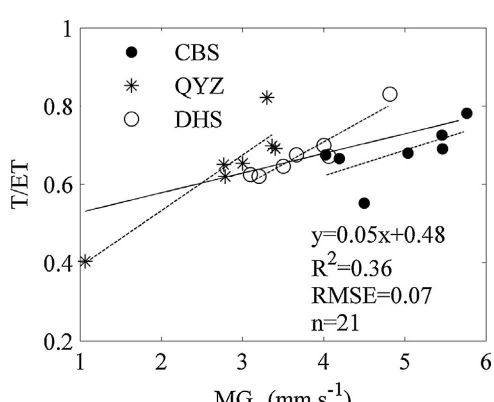

Fig. 11. The relationship between mean annual canopy stomatal conductance (MG$_c$) and annual *T*/ET. *T*/ET was the ratio of the simulated annual total transpiration (*T*) to the annual total evapotranspiration (ET). The dash lines were the interannual variation of *T*/ET at each forest, while the solid line was the regression line between MG$_c$ and *T*/ET among forests.

4.2. Factors affecting the Variations of *T*/ET

The variations of *T*/ET, including the diurnal variation, seasonal variation and so on, can be fulfilled through changing the canopy stomatal conductance (G_c), the soil surface conductance (G_s, the reciprocal of r_{ss} in Eq. (5)), and the portion that the energy absorbed by canopy (P_{EC}, Eq. (8)) (Hu et al., 2009).

The diurnal variation of T/ET was mainly affected by that of G_c as little variation in G_s and P_{EC} during the same day. The variation of G_s and P_{EC} were primarily affected by that of S_{wc} (Eq. (5)) and LAI (Eq. (8)), which showed little variation in the same day, while PAR had obvious diurnal dynamics, which made G_c vary substantially (Stoy et al., 2008) and then the variation of T/ET. Our results were also consistent with the previous study (Hu et al., 2009).

The seasonal variation of T/ET was jointly affected by that of G_c, G_s or P_{EC} but the joint effects differed among ecosystems. The seasonal dynamics of G_c was affected by PAR, VPD, and LAI (Stoy et al., 2008), while that of G_s and P_{EC} were affected by S_{wc} (Eq. (5)) and LAI (Eq. (8)), respectively. At CBS, T_a and LAI experienced obvious seasonal dynamics (Shi et al., 2008a; Zhu et al., 2014), which made G_c and P_{EC} vary substantially among seasons thus hided the effect of G_s on the variation of T/ET. The seasonal dynamics of T/ET was therefore jointly affected by that of G_c and P_{EC} through the direct effects of T_a, VPD, and LAI, which was consistent with previous studies (Hu et al., 2009; Huang et al., 2010; Zhu et al., 2014). At subtropical forests (QYZ and DHS), LAI did not exhibit obvious seasonal variation (Zhu et al., 2014), and the seasonal dynamics of PAR was accompanied with that of T_a, VPD, and R_n, which made G_c vary obviously but P_{EC} vary little. In addition, the seasonal variation of G_s induced by S_{wc} also played an important role in the seasonal dynamics of T/ET as little variation in LAI thus G_c and P_{EC}. Therefore, the seasonal dynamics of T/ET was jointly affected by that of G_c and G_s through the direct effects of T_a, VPD, R_n, and SW, which differed from previous studies at temperate ecosystems (Hu et al., 2009; Huang et al., 2010; Zhu et al., 2014).

At annual scale, T/ET of these three forests were higher than that of grasslands (Hu et al., 2009; Lauenroth and Bradford, 2006) and croplands (Kato et al., 2004), which resulted from the higher LAI (Huxman et al., 2005). The interannual variation and the spatial variation of T/ET were governed by mean annual G_c (MG_c) (Fig. 10).

Therefore, G_c strongly affected the spatial and temporal variations of T/ET in three forest ecosystems of China, including the diurnal variation, the seasonal variation, and the interannual variation, while the seasonal variation of T/ET was also affected by P_{EC} at temperate forest and G_s at subtropical forests.

5. Conclusions

Based on eddy covariance measurements at three forests of ChinaFLUX situated in NSTEC, we run the S–W model, validated its performance with two layer eddy covariance measurements, and analyzed the spatiotemporal variations of T/ET. The S–W model performed well in simulating ET and T/ET but some improvements should be needed in adding EI session in the future. At three forests, T/ET all exceeded 0.6, indicating that vegetation played an important role in regulating the climate, which should be highly emphasized in the future. The spatial and temporal variations of T/ET, including the diurnal variation, the seasonal variation and the interannual variation, were mainly affected by the canopy stomatal conductance, while soil water content played an important role through altering the soil surface conductance in regulating the seasonal dynamics of T/ET at subtropical forests.

Acknowledgements

This research was supported by the Natural Science Foundation of China (Grant 31290221, 31420103917, and 41301043), National Key Research and Development Program (Grant 2010CB833504), the CAS Strategic Priority Research Program (Grant XDA05050601), and Funding for talent young scientists of IGSNRR (Grant 2013RC203). We gratefully acknowledge the reviewers for spending their valuable time to provide constructive comments.

References

Aubinet, M., Grelle, A., Ibrom, A., Rannik, U., Moncrieff, J., Foken, T., Kowalski, A.S., Martin, P.H., Berbigier, P., Bernhofer, C., Clement, R., Elbers, J., Granier, A., Grunwald, T., Morgenstern, K., Pilegaard, K., Rebmann, C., Snijders, W., Valentini, R., Vesala, T., 2000. Estimates of the annual net carbon and water exchange of forests: the EUROFLUX methodology. Adv. Ecol. Res. 30, 113–175.

Beer, C., Ciais, P., Reichstein, M., Baldocchi, D., Law, B.E., Papale, D., Soussana, J.F., Ammann, C., Buchmann, N., Frank, D., Gianelle, D., Janssens, I.A., Knohl, A., Kostner, B., Moors, E., Roupsard, O., Verbeeck, H., Vesala, T., Williams, C.A., Wohlfahrt, G., 2009. Temporal and among-site variability of inherent water use efficiency at the ecosystem level. Global Biogeochem. Cycle 23, GB2018.

Beiderwieden, E., Wolff, V., Hsia, Y.J., Klemm, O., 2008. It goes both ways: measurements of simultaneous evapotranspiration and fog droplet deposition at a montane cloud forest. Hydrol. Processes 22, 4181–4189.

Blyth, E., Harding, R.J., 2011. Methods to separate observed global evapotranspiration into the interception, transpiration and soil surface evaporation components. Hydrol. Processes 25, 4063–4068.

Eugster, W., Burkard, R., Holwerda, F., Scatena, F.N., Bruijnzeel, L.A., 2006. Characteristics of fog and fogwater fluxes in a Puerto Rican elfin cloud forest. Agric. For. Meteorol. 139, 288–306.

Falge, E., Baldocchi, D., Olson, R., Anthoni, P., Aubinet, M., Bernhofer, C., Burba, G., Ceulemans, G., Clement, R., Dolman, H., Granier, A., Gross, P., Grunwald, T., Hollinger, D., Jensen, N.O., Katul, G., Keronen, P., Kowalski, A., Lai, C.T., Law, B.E., Meyers, T., Moncrieff, J., Moors, E., Munger, J.W., Pilegaard, K., Rannik, U., Rebmann, C., Suyker, A., Tenhunen, J., Tu, K., Verma, S., Vesala, T., Wilson, K., Wofsy, S., 2001a. Gap filling strategies for long term energy flux data sets. Agric. For. Meteorol. 107, 71–77.

Falge, E., Baldocchi, D., Olson, R., Anthoni, P., Aubinet, M., Bernhofer, C., Burba, G., Ceulemans, R., Clement, R., Dolman, H., Granier, A., Gross, P., Grunwald, T., Hollinger, D., Jensen, N.O., Katul, G., Keronen, P., Kowalski, A., Lai, C.T., Law, B.E., Meyers, T., Moncrieff, H., Moors, E., Munger, J.W., Pilegaard, K., Rannik, U., Rebmann, C., Suyker, A., Tenhunen, J., Tu, K., Verma, S., Vesala, T., Wilson, K., Wofsy, S., 2001b. Gap filling strategies for defensible annual sums of net ecosystem exchange. Agric. For. Meteorol. 107, 43–69.

Falge, E., Reth, S., Bruggemann, N., Butterbach-Bahl, K., Goldberg, V., Oltchev, A., Schaaf, S., Spindler, G., Stiller, B., Queck, R., Kostner, B., Bernhofer, C., 2005. Comparison of surface energy exchange models with eddy flux data in forest and grassland ecosystems of Germany. Ecol. Modell. 188, 174–216.

FAO, 2010. Global Forest Resource Assessments 2010: Key Findings. FAO, Rome, Italy.

Gao, Y., Yu, G., Yan, H., Zhu, X., Li, S., Wang, Q., Zhang, J., Wang, Y., Li, Y., Zhao, L., Shi, P., 2014. A MODIS-based Photosynthetic Capacity Model to estimate gross primary production in Northern China and the Tibetan Plateau. Remote Sens. Environ. 148, 108–118.

Ge, Z.-M., Zhou, X., Kellomäki, S., Peltola, H., Wang, K.-Y., 2011. Climate, canopy conductance and leaf area development controls on evapotranspiration in a boreal coniferous forest over a 10-year period: a united model assessment. Ecol. Modell. 222, 1626–1638.

Gower, S.T., Kucharik, C.J., Norman, J.M., 1999. Direct and indirect estimation of leaf area index, f(APAR), and net primary production of terrestrial ecosystems. Remote Sens. Environ. 70, 29–51.

Granier, A., Biron, P., Lemoine, D., 2000. Water balance, transpiration and canopy conductance in two beech stands. Agric. For. Meteorol. 100, 291–308.

Hollinger, D.Y., Kelliher, F.M., Byers, J.N., Hunt, J.E., McSeveny, T.M., Weir, P.L., 1994. Carbon-dioxide exchange between an undisturbed old-growth temperate forest and the atmosphere. Ecology 75, 134–150.

Hu, Z.M., Yu, G.R., Fu, Y.L., Sun, X.M., Li, Y.N., Shi, P.L., Wang, Y.F., Zheng, Z.M., 2008. Effects of vegetation control on ecosystem water use efficiency within and among four grassland ecosystems in China. Global Change Biol. 14, 1609–1619.

Hu, Z.M., Yu, G.R., Zhou, Y.L., Sun, X.M., Li, Y.N., Shi, P.L., Wang, Y.F., Song, X., Zheng, Z.M., Zhang, L., Li, S.G., 2009. Partitioning of evapotranspiration and its controls in four grassland ecosystems: Application of a two-source model. Agric. For. Meteorol. 149, 1410–1420.

Huang, X., Hao, Y., Wang, Y., Cui, X., Mo, X., Zhou, X., 2010. Partitioning of evapotranspiration and its relation to carbon dioxide fluxes in Inner Mongolia steppe. J. Arid. Environ. 74, 1616–1623.

Huxman, T.E., Wilcox, B.P., Breshears, D.D., Scott, R.L., Snyder, K.A., Small, E.E., Hultine, K., Pockman, W.T., Jackson, R.B., 2005. Ecohydrological implications of woody plant encroachment. Ecology 86, 308–319.

Iritz, Z., Tourula, T., Lindroth, A., Heikinheimo, M., 2001. Simulation of willow short-rotation forest evaporation using a modified Shuttleworth–Wallace approach. Hydrol. Processes 15, 97–113.

Kang, M., Kwon, H., Cheon, J.H., Kim, J., 2012. On estimating wet canopy evaporation from deciduous and coniferous forests in the Asian monsoon climate. J. Hydrometeorol. 13, 950–965.

Kato, T., Kimura, R., Kamichika, M., 2004. Estimation of evapotranspiration, transpiration ratio and water-use efficiency from a sparse canopy using a compartment model. Agric. Water Manage. 65, 173–191.

Kool, D., Agam, N., Lazarovitch, N., Heitman, J.L., Sauer, T.J., Ben-Gal, A., 2014. A review of approaches for evapotranspiration partitioning. Agric. For. Meteorol. 184, 56–70.
Kume, T., Tanaka, N., Kuraji, K., Komatsu, H., Yoshifuji, N., Saitoh, T.M., Suzuki, M., Kumagai, T.O., 2011. Ten-year evapotranspiration estimates in a Bornean tropical rainforest. Agric. For. Meteorol. 151, 1183–1192.
Lauenroth, W.K., Bradford, J.B., 2006. Ecohydrology and the partitioning AET between transpiration and evaporation in a semiarid steppe. Ecosystems 9, 756–767.
Law, B.E., Van Tuyl, S., Cescatti, A., Baldocchi, D.D., 2001. Estimation of leaf area index in open-canopy ponderosa pine forests at different successional stages and management regimes in Oregon. Agric. For. Meteorol. 108, 1–14.
Lawrence, D.M., Thornton, P.E., Oleson, K.W., Bonan, G.B., 2007. The partitioning of evapotranspiration into transpiration, soil evaporation, and canopy evaporation in a GCM: impacts on land-atmosphere interaction. J. Hydrometeorol. 8, 862–880.
Liu, C., Zhang, X., Zhang, Y., 2002. Determination of daily evaporation and evapotranspiration of winter wheat and maize by large-scale weighing lysimeter and micro-lysimeter. Agric. For. Meteorol. 111, 109–120.
Maestre-Valero, J.F., Ragab, R., Martínez-Alvarez, V., Baille, A., 2012. Estimation of dew yield from radiative condensers by means of an energy balance model. J. Hydrol. 460–461, 103–109.
Menzel, A., Jakobi, G., Ahas, R., Scheifinger, H., Estrella, N., 2003. Variations of the climatological growing season (1951–2000) in Germany compared with other countries. Int. J. Climatol. 23, 793–812.
Reichstein, M., Falge, E., Baldocchi, D., Papale, D., Aubinet, M., Berbigier, P., Bernhofer, C., Buchmann, N., Gilmanov, T., Granier, A., Grunwald, T., Havrankova, K., Ilvesniemi, H., Janous, D., Knohl, A., Laurila, T., Lohila, A., Loustau, D., Matteucci, G., Meyers, T., Miglietta, F., Ourcival, J.M., Pumpanen, J., Rambal, S., Rotenberg, E., Sanz, M., Tenhunen, J., Seufert, G., Vaccari, F., Vesala, T., Yakir, D., Valentini, R., 2005. On the separation of net ecosystem exchange into assimilation and ecosystem respiration: review and improved algorithm. Global Change Biol. 11, 1424–1439.
Scanlon, T.M., Kustas, W.P., 2012. Partitioning evapotranspiration using an eddy covariance-based technique: improved assessment of soil moisture and land-atmosphere exchange dynamics. Vadose Zone J., 11, http://dx.doi.org/10.2136/vzj2012.0025.
Schlesinger, W.H., Jasechko, S., 2014. Transpiration in the global water cycle. Agric. For. Meteorol. 189–190, 115–117.
Shi, T., Guan, D., Wang, A., Wu, J., Jin, C., Han, S., 2008a. Comparison of three models to estimate evapotranspiration for a temperate mixed forest. Hydrol. Processes 22, 3431–3443.
Shi, T.T., Guan, D.X., Wu, J.B., Wang, A.Z., Jin, C.J., Han, S.J., 2008b. Comparison of methods for estimating evapotranspiration rate of dry forest canopy: Eddy covariance, Bowen ratio energy balance, and Penman–Monteith equation. J. Geophys. Res. 113, D19116.
Shuttleworth, W.J., Wallace, J.S., 1985. Evaporation from sparse crops-an energy combination theory. Q. J. R. Meteor. Soc. 111, 839–855.
Stoy, P.C., Katul, G.G., Siqueira, M.B.S., Juang, J.Y., Novick, K.A., McCarthy, H.R., Oishi, A.C., Oren, R., 2008. Role of vegetation in determining carbon sequestration along ecological succession in the southeastern United States. Global Change Biol. 14, 1409–1427.
Stoy, P.C., Katul, G.G., Siqueira, M.B.S., Juang, J.Y., Novick, K.A., McCarthy, H.R., Oishi, A.C., Uebelherr, J.M., Kim, H.S., Oren, R., 2006. Separating the effects of climate and vegetation on evapotranspiration along a successional chronosequence in the southeastern US. Global Change Biol. 12, 2115–2135.
Wang, Y.P., Leuning, R., 1998. A two-leaf model for canopy conductance, photosynthesis and partitioning of available energy I: model description and comparison with a multi-layered model. Agric. For. Meteorol. 91, 89–111.
Webb, E.K., Pearman, G.L., Leuning, R., 1980. Correction of flux measurement for density effects due to heat and water vapor transfer. Q. J. R. Meteor. Soc. 106, 85–100.
Wen, X.F., Wang, H.M., Wang, J.L., Yu, G.R., Sun, X.M., 2010. Ecosystem carbon exchanges of a subtropical evergreen coniferous plantation subjected to seasonal drought, 2003–2007. Biogeosciences 7, 357–369.
Wilson, K.B., Hanson, P.J., Mulholland, P.J., Baldocchi, D.D., Wullschleger, S.D., 2001. A comparison of methods for determining forest evapotranspiration and its components: sap-flow, soil water budget, eddy covariance and catchment water balance. Agric. For. Meteorol. 106, 153–168.
Yan, J., Liu, X., Tang, X., Yu, G., Zhang, L., Chen, Q., Li, K., 2013. Substantial amounts of carbon are sequestered during dry periods in an old-growth subtropical forest in South China. J. For. Res. 18, 21–30.
Yu, G.-R., Zhu, X.-J., Fu, Y.-L., He, H.-L., Wang, Q.-F., Wen, X.-F., Li, X.-R., Zhang, L.-M., Zhang, L., Su, W., Li, S.-G., Sun, X.-M., Zhang, Y.-P., Zhang, J.-H., Yan, J.-H., Wang, H.-M., Zhou, G.-S., Jia, B.-R., Xiang, W.-H., Li, Y.-N., Zhao, L., Wang, Y.-F., Shi, P.-L., Chen, S.-P., Xin, X.-P., Zhao, F.-H., Wang, Y.-Y., Tong, C.-L., 2013. Spatial patterns and climate drivers of carbon fluxes in terrestrial ecosystems of China. Global Change Biol. 19, 798–810.
Yu, G.R., Song, X., Wang, Q.F., Liu, Y.F., Guan, D.X., Yan, J.H., Sun, X.M., Zhang, L.M., Wen, X.F., 2008. Water-use efficiency of forest ecosystems in eastern China and its relations to climatic variables. New Phytol. 177, 927–937.
Zhang, J.H., Han, S.J., Yu, G.R., 2006. Seasonal variation in carbon dioxide exchange over a 200-year-old Chinese broad-leaved Korean pine mixed forest. Agric. For. Meteorol. 137, 150–165.
Zhu, X., Yu, G., Wang, Q., Hu, Z., Han, S., Yan, J., Wang, Y., Zhao, L., 2014. Seasonal dynamics of water use efficiency of typical forest and grassland ecosystems in China. J. For. Res. 19, 70–76.